GEOMATICS, NATURAL HAZARDS AND RISK
2018, VOL. 9, NO. 1, 862–880
https://doi.org/10.1080/19475705.2018.1475426

Taylor & Francis
Taylor & Francis Group

RESEARCH ARTICLE

OPEN ACCESS Check for updates

Classification, grading criteria and quantitative expression of earth fissures: a case study in Daming Area, North China Plain

Jishan Xu[a], Jianbing Peng[b,c,d], Yahong Deng[b], Hongqian He[e], Lingchao Meng[e] and Feiyong Wang[b]

[a]School of Resources and Geosciences, China University of Mining and Technology, Xuzhou, Jiangsu, China; [b]School of Geology Engineering and Geomatics, Chang'an University, Xi'an, ShaanXi, China; [c]Institute of Geo-hazards Mitigation, Chang'an University, Xi'an, ShaanXi, China; [d]Key Laboratory of Western Mineral Resources and Geological Engineering Ministry of Education, Chang'an University, Xi'an, ShaanXi, China; [e]North China University of Water Resources and Electric Power, Zhengzhou, Henan, China

ABSTRACT

Observation, description and preliminary analysis are important means in studies on earth fissures. As a phenomenon of surface fractures, earth fissures are formed under the joint action of exogenetic and endogenetic forces and their development can be characterized by parameters of length, width, depth, fractal dimension and influential width. Based on their length, we deduced a 'length-grade conversion equation' and divided earth fissures into 10 grades. In addition, we also deduced a series functions to describe the contribution of fissure-inducing forces including active fault, earthquake, groundwater withdrawal and ancient river channels based on their roles in fissure formation and their affecting conditions. These functions provide the criteria for classification of earth fissures. In order to verify the effectiveness of these methods, we took Daming fracture zone on the North China Plain as an example to quantitatively calculate the control factors of the earth fissures in this area. Moreover, we proposed various plane expression methods for single and grouped earth fissures that could be used to improve the relevant studies on earth fissures.

ARTICLE HISTORY
Received 25 December 2017
Accepted 2 May 2018

KEYWORDS
Earth fissure; grading criteria; quantitative method; controlling factor; North China Plain

1. Introduction

Earth fissures are produced by the interaction of different geological forces applied on shallow surface strata, and linear manifestations of soil–rock body fractures on ground surface (Peng 2013 ; Deng et al. 2013). Like other fracture tectonics, the science of earth fissures is a geometrical morphological study deducing the causes from

CONTACT Jishan Xu xujs@cumt.edu.cn; Jianbing Peng dicexy_1@chd.edu.cn

appearances of earth fissures. The observation of natural phenomena is the first step to a scientific theory, beginning from problems but focusing on how to explain them. For instance, there are many longer earth fissures (up to 15 km) in the structural basin in the southwestern United States (Arizona State), but there are also many shorter earth fissures (generally a few hundred metres) (Carpenter 1993). In order to directly reflect the relationship between earth fissures and their controlling factors (fault, earthquake or groundwater pumping), some researchers portrayed them as 'dots' on a planar graph, ignoring their directionality and assuming they are distributed roughly along the bedrock area (Jachens and Holzer 1982). Others noted that the earliest date of earth fissures (13 November 1927) is very similar to the date recording the earthquake by the Arizona Tree Ring Laboratory photographs (11 September 1927) (Leonard 1929). Therefore, they believed that seismic activity is the dominant factor. With further study, more and more scholars use painstaking 'lines' to describe these earth fissures. They even analysed stratigraphic profiles and found that these earth fissures appear to be dynamic and are more closely related to atmospheric precipitation and groundwater pumping activities (Heindl et al. 1955; Pashley 1961; Carpenter 1993). Because these factors affect earth fissures and their characteristics emphasize different aspects, studies on these factors often lead to different judgments on the same geological phenomenon and even opposite conclusions.

In Xi'an, Shaanxi province, China, 14 typical earth fissures have been developed. These fissures are arranged in parallel and equidistant to the north of Lintong-Chang'an fault with an average length of about 12 km (Peng et al. 2016). As early as the beginning of the study (1970s), the researchers noticed and used a drawing method to truthfully and accurately describe the characteristics of these earth fissures in plane and section and found that their formation and fracture activity have a specific 'syngenetic mechanism' (Wang 2016). Other researchers have long-term monitored Xi'an area using GPS survey and levelling measurements from 2005 to 2012 and found that earth fissures have undergone specific dynamic development process as manifested as land subsidence at average of 50 mm/yr (Qu et al. 2014). Based on this, we have concluded that earth fissures in Xi'an may have undergone a 'disaster chain' process from mining groundwater to land subsidence to earth fissures (Xu et al. 2016). Using theoretical modelling methods, it is also possible to link the development of earth fissures to active faults, even deep structures and reveal the response of the earth's surface to the tectonic movement on the scale of plate tectonic basin (Weihe Basin) (Peng 2014; Peng et al. 2016). Overall, research on earth fissures at different scales may lead to discrepancy in understanding the phenomenon.

Till now, the phenomena of earth fissures have been found in many countries and regions around the world. For example, nearly 368 earth fissures have been found in the valley area of Mexico (Rodríguez et al. 2006; Auvinet et al. 2010), 23 earth fissures in the Wadi Al-Yutamah valley in western Saudi Arabia (Bankher and Al-Harthi 1999), and more in the southeast Plains, African Rift, European Plains, etc. All these fissures are different in types, sizes and characteristics (Haimson and Rummel, 1982; Nutalaya et al., 1996; Ayalew et al. 2004; Phienwej et al., 2006). These fissures spatially extend in linear form with scales smaller than faults and undergo static activities (destruction degree) smaller than earthquakes. Using other geological phenomena

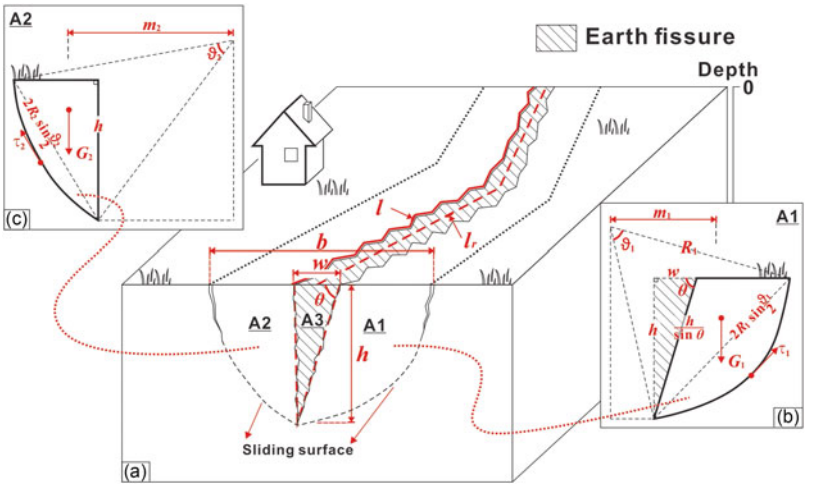

Figure 1. Three-dimensional structure of earth fissure. A1, A2-shear zones; A3-tensile zone. In this figure, l_r is the measured length of the fissure, l is the actual length, w is the width of the fissure, b is the influence width, h is the depth of the fissure and θ is the dip of fault.

such as faults to characterize earth fissures will cause distortion and confusion. Thus, a unique expression pattern is needed to describe earth fissures in a scientific, appropriate and approximate way.

In this study, we try to answer three core questions. First, what are the parameters reflecting the essential characteristics of earth fissures and how to express them quantitatively for a particular earth fissure? Second, how to obtain and classify the factors dominantly affecting the development of stratigraphic structure, tectonic activities, groundwater activities, etc.? Third, how to, based on the essential characteristics of earth fissures, build a reasonable scheme to classify and reflect these factors on maps with various geological information? Our research on these problems can provide a foundation for quantitatively study on single earth fissures and a useful method and thought for study on regional even global earth fissures.

2. Quantitative description of earth fissures

As a surface fracture appearance of soil–rock mechanical behaviours, the morphology of earth fissures reflects some type(s) of exogenetic or endogenetic forces (Zhang et al. 2008). Generally, the 'fissure-generating force' accumulated in certain range and depth of soil–rock layers often manifests on ground surface as individual mechanical behaviours including extending along its strike, inclination and vertical directions as well as the total number of fissures in nearby areas. Overall, earth fissures can be quantitatively described using the following parameters, including length (l), width (w), depth (h), fractal dimension (D) and influencing width (b) (Figure 1).

It should be noted that the actual length of earth fissures is related to the degree of its zigzagness. It can be found in the regional survey that the morphology of earth fissures is fractal. Assuming that the measurement standard is r and the corresponding measured length and fractal dimension of earth fissures is l_r and D, respectively,

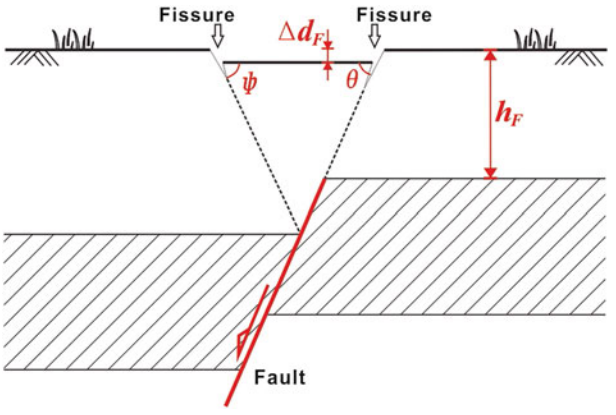

Figure 2. Contribution of fault activity to earth fissures.

then

$$l = l_r = N \cdot r^{1-D} \tag{1}$$

Taking logarithm on both sides of Eq. (1) we obtain

$$\ln l_r = (1-D) \ln r + N' \tag{2}$$

where N and N' are unknown coefficient. It is clear that Eq. (2) describes a linear graphic with slope of (1 – D). Therefore, the fractal dimension (D) of earth fissures can be obtained and it actually reflects the zigzag degree of earth fissures.

The depth (h) is defined as the downward extending depth of fissure activity, rather than the maximum potential extending scale. Similarly, the width here is the average original width without external force disturbance, but not the 'visible width'. This is because the reconstruction by external disturbances (e.g. irrigation, precipitation, gravity-induced collapse or weathering action) is a secondary shaping effect on earth fissures, and is already deviated from the initially triggered static tensile–fracture behaviours.

It is particularly important to note the difference between 'fissure width (W)' and 'influencing width (B)'. In general, earth fissure activity can result in two types of rupture areas near the surface soil – the shear zone (Figure 1, A1 and A2) and the stretching zone (Figure 1, A3). The width of the surface rupture zone is denoted as b_{A3} ($b_{A3} = w$). Assuming the inclination angle of the earth fissure rapture surface is θ, it is true that

$$b_{A3} = w = \frac{h}{\tan\theta} \tag{3}$$

The shear zone consists of two parts (Figure 1, A1 and A2). Their corresponding surface intervals are their influencing widths and denoted as b_{A1} and b_{A2}. For the shear zone A1, it is assumed that the shear plane is a circular arc with a radius of R_1 and an arc of ϑ_1. Assuming that the gravity of the potential slider is G_1, the distance from the moment centre to the arc is m_1. The shear strength of the soil, τ_1,

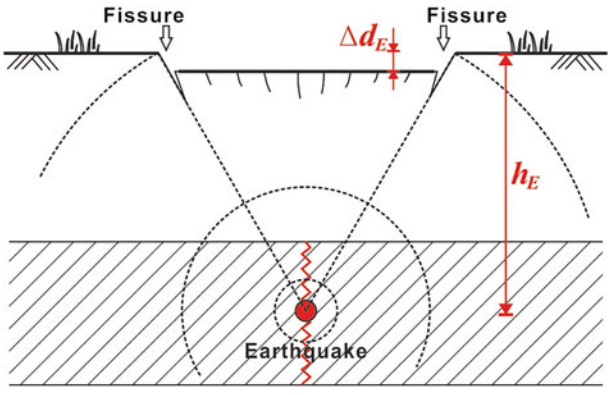

Figure 3. Contribution of earthquake activity to earth fissures.

is the force to prevent sliding. Assuming that the slope is in limit equilibrium state, it holds

$$\tau_1 \cdot \vartheta_1 \cdot R_1 = G_1 \cdot m_1 \tag{4}$$

Since the arc-shaped sliding surface is calculated by several attempts, the parameters R_1, ϑ_1 and m_1 are mutually corresponding and known. Therefore,

$$R_1 = \frac{G_1 \cdot m_1}{\tau_1 \cdot \vartheta_1} \tag{5}$$

As shown in Figure 1(b), the fissure width (b_{A1}) corresponding to the shear zone A1 can be obtained according to the cosine theorem, i.e.

$$b_{A1} = -h \cot\theta + \sqrt{\left(2R_1 \sin\frac{\vartheta_1}{2}\right)^2 - h^2} \tag{6}$$

Likewise, the corresponding sliding surface arc length R_2 of the shear zone A2 can be obtained as

$$R_2 = \frac{G_2 \cdot m_2}{\tau_1 \cdot \vartheta_2} \tag{7}$$

As shown in Figure 1(c), the section of the rupture zone is a right-angled triangle. According to the Pythagorean theorem, the fracture width b_{A2} corresponding to the shear zone A2 can be obtained as

$$b_{A2} = \sqrt{\left(2R_2 \sin\frac{\vartheta_2}{2}\right)^2 - h^2} \tag{8}$$

The rupture width of the earth fissures is the sum of the rupture widths corresponding to the stretching zone (A3) and the shear zone (A1, A2). Therefore,

$$b = b_{A1} + b_{A2} + b_{A3} = -h\cot\theta + \sqrt{\left(2R_1\sin\frac{\vartheta_1}{2}\right)^2 - h^2} + \sqrt{\left(2R_2\sin\frac{\vartheta_2}{2}\right)^2 - h^2} + w \tag{9}$$

When the inclination of the main crack surface (Figure 1, A3) is upright and closed (i.e. $\theta = \pi/2$, $w = 0$), $R_1 = R_2$, $\vartheta_1 = \vartheta_2$ the formula can be further simplified as

$$b = \sqrt[2]{\left(2R_1\sin\frac{\vartheta_1}{2}\right)^2 - h^2} \tag{10}$$

Above analyses showed that earth fissures are three-dimensional in shape. During deformation and failure, they are subjected to volumetric changes. The traditional classifications and grading methods are based on length and do not consider the differences in width or depth, which is obviously unreasonable. Thus, earth fissures need to be measured using 'fissure zone' volume (V_w) and 'fissure influencing zone' volume (V_b). For the earth fissure shown in Figure 1, the 'fissure zone volume' (V_w) can be expressed as

$$V_w = \frac{1}{2}\cdot w\cdot h\cdot l \tag{11}$$

If taking the boundary of the influencing zone, sliding band, as a straight line, the 'fissure influencing zone' volume (V_b) can be expressed approximately as

$$V_b \approx \frac{1}{2}\cdot b\cdot h\cdot l \tag{12}$$

The depths (h) of earth fissures are hardly observable in field investigations and the fissure width (w) in large-scale development is approximate same, let

$$\frac{h\cdot w}{2} \approx C \tag{13}$$

where C is a constant. The formula (12) can be expressed as

$$V_b = C\cdot l \tag{14}$$

It is obvious that the length-based criterion of earth fissure classification is an approximate expression. Since many parameters are unknown in field investigations, a simpler approach is needed in expression and description of earth fissure. On the other hand, as for regional distribution, the characteristic parameters of earth fissures are similar to some extent. Thus, the length-based classification criterion has some values and significance for studying the unknown and regional earth fissures.

3. Classification and grading of earth fissures

3.1. Classification

Grading and classification of geological phenomena is the crucial process of summarizing and extracting their main characteristics and is the foundation of theoretical research. Earth fissures are classified based on their characteristics (Jingming 2000), and their development is affected by many factors including fault activity, historical earthquake activity, groundwater extraction and buried ancient river channels (Dou et al. 2005; Wang et al. 2009; Zhang et al. 2012; Chen et al. 2014; Brunori et al. 2015).

From the above analysis, it is clear that the damages caused by various affecting factors to the near-surface soil are presented in three-dimensional topographic forms (impacting volume, V_b). Assuming that the impact on the earth soil results in a certain amount of soil displacement, Δp, i.e. the equivalent displacement rather than the actual displacement (Because only a limited number of factors are considered here), the energy, J_0, of the resulted earth fissure can be obtained using the following equation:

$$J_0 = V_b \cdot \gamma \cdot \Delta p = \frac{1}{2} bhl \cdot \gamma \cdot \Delta p \tag{15}$$

where γ is the average bulk density of the soil body. For a particular earth fracture, assuming that the energy consumed by various affecting factors during the formation of an earth fissure is J_F for fault activity, J_E for seismicity, J_W for groundwater extraction and J_R for ancient river channel distribution, respectively, their contribution to the earth fissure formation can be obtained by comparison of J_F, J_E, J_W and J_R with J_0.

$$K_F = \frac{J_F}{J_0} \cdot 100\% \tag{16}$$

$$K_E = \frac{J_E}{J_0} \cdot 100\% \tag{17}$$

$$K_W = \frac{J_W}{J_0} \cdot 100\% \tag{18}$$

$$K_R = \frac{J_R}{J_0} \cdot 100\% \tag{19}$$

They have the following relation

$$K_F + K_E + K_W + K_R \approx 1 \tag{20}$$

Obviously, the controlling factors of an earth fissure are related to the magnitudes of their contributions to the formation of the earth fissure (K_i, $0 \leq K_i \leq 1$ and

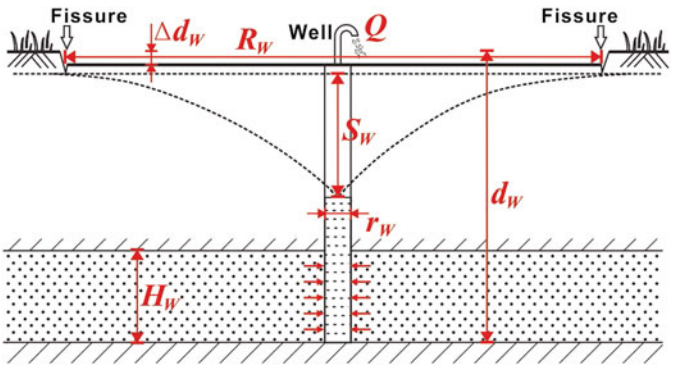

Figure 4. Contribution of groundwater extraction to earth fissures.

$\Sigma K_i = 1$). When the contribution of a factor is greater than 50% or much greater than those of other factors, the factor is the main control factor for the formation of the earth fissure.

As shown in Figure 2, for the fault factor, its main parameters affecting the development of earth fissures include its inclination, burial depth and activity. The fault's activity in the deep soil body will cause its overlying soil body to fissure, which is equivalent to the vertical uniaxial compression shear failure with rupture angle of ψ

$$\psi = \frac{\varphi}{2} + \frac{\pi}{4} \tag{21}$$

where φ is the internal friction angle of the soil. Assuming that the vertical displacement of the ruptured soil caused by the fault activity is Δd_{F}, the work done by the fault on the soil in the earth fissure zone is further found to be

$$J_{\mathrm{F}} = \frac{1}{2}(\cot\theta + \cot\psi) h_{\mathrm{F}}^2 l \cdot \gamma \cdot \Delta d_{\mathrm{F}} \tag{22}$$

where J_{F} is the energy of the earth fissure.

For the seismic factor as shown in Figure 3, it is assumed that the surface rupture caused by an earthquake with the focal depth of D and the Gutenberg magnitude of M forms a belt-like earth fissure in the strike of the fault, using historical earthquake statistical data in North China can separately find the relationships of the earth fissure length, width and dislocation to the seismic magnitude (Deng et al. 1987; Guo, 2000) as follows:

$$M = 0.88 \log l + 5.92 \tag{23}$$

$$M = 0.35 \log b_{\mathrm{E}} + 6.05 \tag{24}$$

$$M = 0.68 \log \Delta d_{\mathrm{E}} + 7.13 \tag{25}$$

It is worthy to note that the effect of seismicity on soil rupture weakens rapidly with time. Assuming that the time of the earthquake is t_0 (year), the duration of the

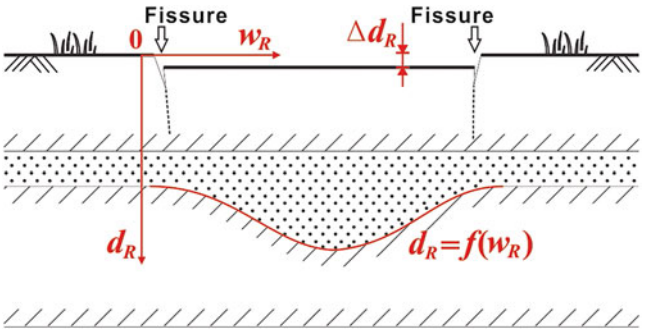

Figure 5. Contribution of buried river channel to earth fissures.

earth fissure caused by it is Δt. If this process conforms to an exponential decay function, its attenuation factor $\eta(t)$ is expressed as

$$\eta(t) = \begin{cases} 1, |t_0 < t < t_0 + \Delta t \\ a_{\mathrm{E}}{}^{t-(t_0+\Delta t)}, |t \geq t_0 + \Delta t \end{cases} \tag{26}$$

where a is a constant. Therefore, the work consumed by the earthquake for the formation of the earth fissure is

$$J_{\mathrm{E}} = \frac{1}{2} b_{\mathrm{E}} h_{\mathrm{E}} l \cdot \gamma \cdot \Delta d_{\mathrm{E}} \cdot \eta(t) \tag{27}$$

For the groundwater extraction, as shown in Figure 4, assume that groundwater extraction from wells forms a circular area with the radius of R_{W}. Taking a complete well in the confined aquifer as an example, let the water level of the well caused by extraction lowers by S_{W}, the flow rate of the pumped well Q, the thickness of the aquifer H_{W}, the permeability coefficient K_{W}, the radius of the well r_{W}, employing the Dupuit formula can find r_{W} as follows:

$$R_{\mathrm{W}} = r_{\mathrm{W}} \cdot \exp\left(\frac{2\pi K_{\mathrm{W}} H_{\mathrm{W}} S_{\mathrm{W}}}{Q}\right) \tag{28}$$

Assuming the earth subsidence due to groundwater withdrawal is Δd_{W}, the well depth from the surface to the well bottom is d_{W}, and the extraction-affected area is approximately a cone, the work done by groundwater extraction can be found as follows:

$$J_{\mathrm{W}} = \frac{2}{3} \pi R_{\mathrm{W}}^2 d_{\mathrm{W}} \cdot \gamma \cdot \Delta d_{\mathrm{W}} \tag{29}$$

The buried ancient river channels, as shown in Figure 5, have uneven geological structure and often are filled with loose sediments. Thus, the actions of gravity and other hydraulic pressures easily result in the fracture of the earth surface. Assume that the burial depth of the river channel is d_{R}, the length and width of the river channel l_{R} and w_{R}, respectively. If the earth surface is used as the abscissa and the

Table 1. Length-based grading of earth fissures.

Class	Grade	Length range (m)
Less than 200 m	1	$l \leq 100$
	2	$100 < l \leq 200$
Hundreds of meters	3	$200 < l \leq 500$
	4	$500 < l \leq 1{,}000$
Thousands of meters	5	$1{,}000 < l \leq 2{,}000$
	6	$2{,}000 < l \leq 5{,}000$
	7	$5{,}000 < l \leq 10{,}000$
A dozen kilometres	8	$10{,}000 < l \leq 22{,}500$
Tens of kilometres	9	$22{,}500 < l \leq 50{,}000$
More than 50km	10	$l > 50{,}000$

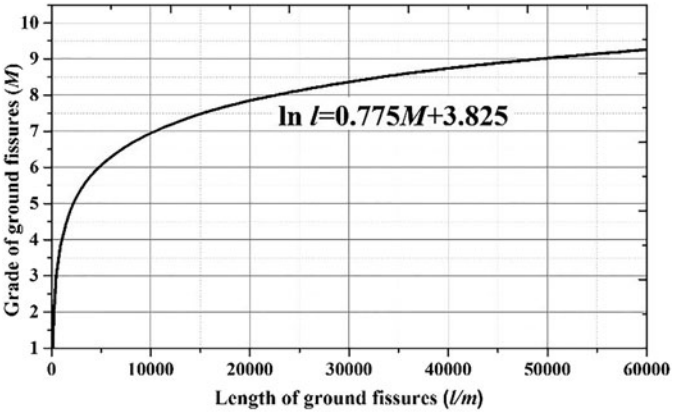

Figure 6. Relationship of fissure length with grade.

'valley shoulder' direction of vertical river channel as the ordinate, a function equation of the bottom boundary of the river channel can be established

$$d_R = f(w_R) \tag{30}$$

Let Δd_R be the vertical dislocation of the earth fissure caused by river channel factors, the work done by the river channel factor in the formation of the earth fissure can be obtained as

$$J_R = \int_0^{w_R} f(w_R) dw_R \cdot l_R \cdot \gamma \cdot \Delta d_W \tag{31}$$

Thus, for a certain specific earth fissure, based on the independent calculations of J_F, J_E, J_W, J_R and J_0, comparing and analysing all the calculated contribution values can finally determine the factors for controlling the formation of earth fissures.

3.2. Grading of earth fissures

The grading of earth fissures is another important issue in this study. Grading earth fissures is by means of some criteria to artificially divide the same type of geological phenomena with different characteristic degrees (e.g. length or intensity). The most

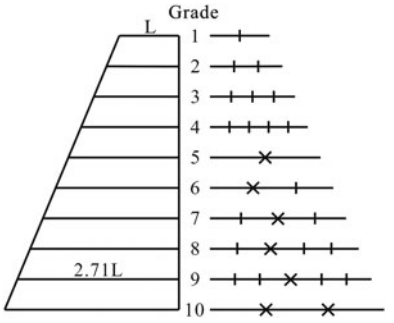

Figure 7. Expressions of line segment legends of earth fissures.

significant characteristic of an earth fissure is its length. Although the length cannot be used as the only parameter to represent earth fissures, using it to divide earth fissures is particularly important in the macroscopic area researches. According to long-term and global surveys, some earth fissures are <100 m long, some are up to 40 km long (Li et al. 2000; Xu et al. 2012), few are >50 km and most are several hundreds of metres to a dozen kilometres long. In general, earth fissures with length ≤100 m are considered as grade 1 and those with length >50 km as grade 9. Based on the energy-grade equation for earthquakes (Gutenberg and Richter 1936), the equation for grading earth fissures can be set as

$$\ln l = x \cdot M + y \tag{32}$$

where M is the grade of the earth fissure, x and y are constant and l is the length of the earth fissure. Separately bringing two groups of data ($x = 1$, $l = 100$) and ($x = 9$, $l = 50{,}000$) into Eq. (32) finds

$$\ln l = 0.775M + 3.825 \tag{33}$$

In other form, it is

$$M = \frac{\ln l - 3.825}{0.775} \tag{34}$$

According to Eq. (34), all earth fissures can be divided into 10 grades. Table 1 and Figure 6 show the correlation between the length and grade of earth fissures.

4. Planar expressions of earth fissures

There are two ways for planar expression of geological phenomena. One is the equi-ratio representation method employed in dealing with faults, terrains or topography, that is, using the same scale as that used in the map to process the geological objects into corresponding point, line and surface symbols so as to find or decode their relative sizes and positions. The other is an indirect method or the grading method, i.e. using a criterion to group certain geological phenomena based on its continuous state (e.g. the energy released by an earthquake) into several grades and indirectly showing

Table 2. Statistics of the main earth fissures in Daming, China.

No.	Location	L. (m)	Tr. (°)	t_i' (°)	Latitude (°)	Longitude (°)	Year
P01	Liweihou	200	8	5	36°16′13″	115°05′45″	1996
P02	Beizhang	560	60	65	36°11′39″	115°08′54″	2010
P03	Zhagner	50	0	5	36°27′49″	115°07′45″	1998
P04	Dongfang	10	75	75	36°22′35″	115°18′15″	1997
P05	Xisong	170	27	25	36°23′57″	115°19′17″	2004
P06	Huaerzhuang-1	500	340	345	36°15′24″	115°15′44″	1981
P07	Huaerzhuang-2	200	85	85	36°15′25″	115°15′45″	1981
P08	Dongxiaotan	200	50	55	36°21′06″	115°18′34″	1988
P09	Qianmo	100	20	25	36°22′42″	115°09′33″	2007
P10	Miaoercun-1	10	15	15	36°13′30″	115°14′16″	2008
P11	Miaoercun-2	100	320	325	36°13′32″	115°14′09″	2008
P12	Miaoercun-3	20	70	75	36°13′33″	115°14′13″	2008
P13	Miaoercun-4	10	285	285	36°13′34″	115°14′22″	2008
P14	Miaosicun-1	100	295	295	36°13′53″	115°14′28″	2010
P15	Miaosicun-2	30	40	45	36°13′50″	115°14′30″	2010
P16	Miaosicun-3	20	40	45	36°13′49″	115°14′34″	2010
P17	Chenzhuang	100	50	55	36°23′28″	115°03′28″	1998
P18	Qianhaizi	500	290	295	36°23′47″	115°05′28″	1998
P19	Xiaolining	10	60	65	36°26′02″	115°00′20″	2010
P20	Xinzhai	20	80	85	36°25′09″	115°03′20″	2007
P21	Xihan	20	25	25	36°18′04″	115°06′50″	2003
P22	Weicun	30	0	5	36°22′40″	115°07′40″	1998
P23	Wanzhong	400	30	35	36°23′15″	115°11′09″	1996
P24	Muyuzhuang	500	345	345	36°25′21″	115°06′42″	1988
P25	Huangjindi	50	330	335	36°27′02″	115°11′21″	1988
P26	Douzhuang	30	335	335	36°21′32″	115°06′52″	2007
P27	Cuizhuang	50	340	345	36°27′10″	115°16′43″	2008
P28	Cuiyue	300	345	345	36°23′07″	115°15′24″	1980
P29	Miaozhuang	1000	5	5	36°22′14″	115°16′42″	2002

the distinguishable images or legends in the map. It is necessary to first compare symbols and legends in the map and then convert them by the preset criterion when using the second method to decode the geological maps.

4.1. Single earth fissure

Researches on earth fissures should not only truly reflect their spatiotemporal distributions but also comprehensively uncover the information of other related geological phenomena, such as faults, epicentre, terrains, topography and the like. Thus, it is necessary for us to represent earth fissures with both a definite distinguishability for themselves and obvious differences from other geological phenomena. Both earth fissures and faults are the geological phenomena with linear extension on their relevant planes (Fan et al. 2004), but the latter are much larger than the former in the spatial scale. Generally, earth fissures are a dozen kilometres long, and faults stretch several hundreds to thousand kilometres, about 10- to 100-fold of the former. Thus, due to the restriction of the map size, representing the faults and the earth fissures in the same map with the same scale will make earth fissures difficult to distinguish. For another geological phenomenon, earthquakes, they are graded and shown by a series of different sizes of circles, 'O', as shown in Figure 7. Therefore, earth fissures are often presented using an equidistant division method of trapezoid with two non-parallel sides. The procedure is as follows:

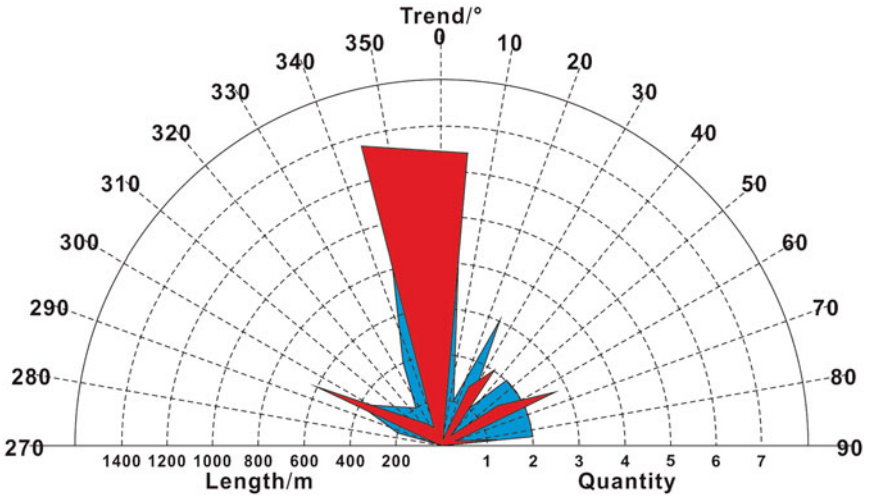

Figure 8. Distribution of length and quantity of earth fissures in Daming, China.

1. Take the legend length of Grade 1 earth fissure, L^1 (L), as the length of the top-side of the trapezoid. Because the real length of Grade 9 earth fissures is dozens of times greater than that of grade 1 fissures, in order to clearly show both of them on the map, the legend length of Grade 9 fissures is given in the following equation:

$$L^9 = e \cdot L^1 \approx 2.71L^1 \tag{35}$$

2. Use the obtained length as the length of the bottom side of the trapezoid and assign $2.71L^1$ as its dimensionless length.
3. Connect the right ends of both the top and bottom sides at a right angle, then connect their left ends, forming a rectangular trapezoid as shown in Figure 7.
4. Divide the vertical right-angle side into eight equidistant sub-trapezoids, producing nine horizontal linear segments as the legend lengths of Grades 1 to 9, and obtain the legend length of Grade 10 fissure through the equal ratio extension as shown in Figure 7.

In order to more clearly distinguish earth fissures from faults on the map and more efficiently judge the grades and length ranges of earth fissures, we assigned different symbols to earth fissures with different grades, as shown in Figure 7. For example, '−+−' is assigned for Grade 1 earth fissures and '−×−' for Grade 5 ones. Because these symbols are artificially designed and not correlated to their real length ranges, the midpoints of these line segments are specified as the real centres of the earth fissures on the map. On the other hand, the direction of the line segment represents the strike of the earth fissure. In this way, all the grades, lengths and distributions of earth fissures can be obtained by counting the number of these 'symbols' on the map.

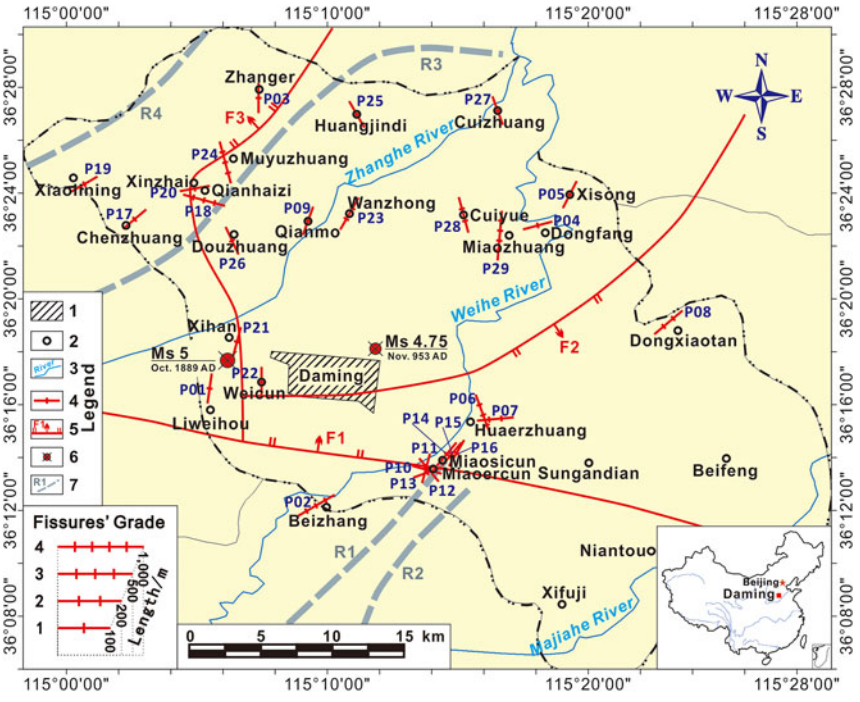

Figure 9. Distribution of earth fissures in Daming, China. 1-county town; 2-villages; 3-river; 4-earth fissures; 5-fault; 6-earthquakes; 7-buried ancient river channel; F1-Cixian-Daming fault; F2-Guanxian fault; F3- Guantao fault.

4.2. Earth fissure combinations

The combinations of earth fissures, such as the North China Plain fissure zone (Jishan et al. 2015), Fen-Wei fissure belt, Xi'an fissure group and the like, can be subdivided into zones, belts, groups and strips. How to compute the predominant direction of the combined earth fissures is another issue. Assuming that in a certain specific region develop n earth fissures with different features but same origination (e.g. they are planar damages due to groundwater extraction or seismic activity), they are marked as $P(l_i, t_i)$ $(0 < i \leq n$ and $i \in N^+)$ according to their lengths (l_i) and strikes $(t_i, 270 \leq t_i < 360$ or $0 \leq t_i < 90)$ as their characteristics.

For statistical simplification, all earth fissures with similar strikes can be assigned as a group. Thus, the whole range of fissure strikes (180°) can be divided into 18 groups at the angle interval of 10°. The average strike of this interval is

$$t_i' = 10 \cdot \left[\frac{t_i}{10}\right] + 5 \tag{36}$$

Obviously,

$$t_i' = 5 \cdot (2\eta - 1) \tag{37}$$

where $1 \leq \eta < 9$ or $27 \leq \eta < 36$.

For a specific t_i' earth fissure with constant length, statistically counting the lengths of all earth fissures in the corresponding l_i group can obtain their accumulated length L_x. The maximum of L_x is the predominant length, that is,

$$L_{\max} = \max L_x = \max \sum l_i \tag{38}$$

Accordingly, the t_i' direction of the predominant length is the predominant strike of the fissure group or all fissures in this group. If there are multiple groups or more than two groups with similar strikes in this region, the group has multiple predominant strikes.

5. Case study

The Daming earth fissure zone was taken as our study subject. The zone lies in the southern end of Hebei Plain, harbouring about 29 earth fissures distributing over more than 20 villages (Table 2). Among these fissures, the longest one is about 1,000 m and the shortest one is 10 m only. Precisely describing these fissures and their spatial relations using fracture factors, such as active faults, ancient river channels, historical earthquakes, was the first task at the description stage. According to the method mentioned above (Figure 7; Table 1), these fissures were classified into four grades (Grades 1 to 4). Their dominant strikes were 5° and 345° and predominant length was 1,000 m (Figure 8).

As shown in Figure 9, six earth fissures denoted as P11–P16 formed a fissure group. They were affected by active fault (F1) and shallow-buried ancient river channel (R1). Field survey found that the zone-affecting region was about 6,000 m wide and about 3–10 m deep (10 m was used for calculation) and had vertical subsidence of about 14.1 mm (4.7 mm/a, 2008–2010) (Zhang et al. 2016). According to Eq. (15), the work required for creating the fissure zone can be estimated as $J_0 = 846l\gamma$.

Survey data showed that the ancient river channel in the zone (R1) was about 5,000–20,000 m wide and had burial depth of about 8–50 m (5,000 m, 8 m were used for calculation in order to calculate the minimum contribution value) and ground subsidence of $\Delta d_R = 14.1$ mm (Wu 2008). Its bottom boundary was relatively flat (approximately a straight line). According to Eq. (31), the work the ancient river channel contributed for the formation of the fissure was estimated as $J_R = 564l\gamma$.

In addition, the Cixian-Daming fault (F1) located in the zone had dip of 50°–60° (55° was used for calculation), minimum burial depth of 5.5–101 m (101 m was used for calculation), breaking activity rate of 0.01–4 mm/a (0.01 mm/a was used for calculation) (Xu 2008) and internal friction angle of 30°. According to Eq. (22), the work that the active fault way contribute for the formation of the fissure was estimated as $J_F \approx 65l\gamma$.

Similarly, according to the results of the pumping test, the radius of the well is 0.5 m, the water level of the well is 15 m, the flow rate is 45 m^3/hr, the thickness of the aquifer is 2 m, the permeability coefficient is 1.5 m/hr, the well depth (d_W) is 25 m and the earth subsidence is 1.5 cm (0.015 m). Assuming the influence radius (R_W) of groundwater extraction is approximately equal to the length (l) of the fissure ($R_W \approx$

l), and according to Eqs. (28) and (29), the work done by groundwater extraction can be estimated as $J_W \approx 210l\gamma$.

Overall, the contribution rate of the ancient river channel K_R and the contribution rate of the active fault K_F were

$$K_R = \frac{564l\gamma}{846l\gamma} \approx 67\% > 50\% \tag{39}$$

$$K_F = \frac{65l\gamma}{846l\gamma} \approx 8\% \tag{40}$$

$$K_W = \frac{210l\gamma}{846l\gamma} \approx 25\% \tag{41}$$

$$K_R + K_W + K_F \approx 1 \tag{42}$$

$$K_R > K_W > K_F \tag{43}$$

The above results indicated that the control factor for formation of the earth fissures in this zone was the buried ancient river channel rather than the active fault.

6. Discussion and conclusions

The studies on earth fissures start from abstracting natural phenomena into linear features followed by observation including classification, summarization, description and representation. As a kind of disaster phenomenon characterized by the rupture of the surface or near surface soil, earth fissure is very sensitive and complicated because of all kinds of geological factors and human factors. Its controlling factors are not as obvious as the macro disasters such as earthquakes and landslides. How to use a criterion to materialize researches into some achievements with physical and geometrical shapes becomes essentially important.

Through the above theoretical deduction and case analysis, it can be seen that the contribution value of each factor (related earth fissures) can be quantitatively calculated using this series of methods mentioned in this study. This is of great scientific value for determining the types of earth fissures and accurately describing the spatial morphology and development characteristics of them. In this study, we analysed this basic issue and made the following conclusions.

1. The objective geological information is expressed using infinite sets and the descriptive geological information is expressed using finite sets composed of a small amount of elements. These two sets are related to each other and their trueness can be measured using the concept of fidelity.
2. The morphology of earth fissures is defined as the fault activities in a three-dimensional space. Accordingly, the development of earth fissures can be characterized by its length, width, depth, fractal dimension and influencing width, and

is represented as volume change. Because width, depth, fractal dimension and influencing width have concealment and similarity, its length is used as a criterion to measure the grade of fissures.

3. Fissure development is controlled by both exogenetic and endogenetic forces, including fault activity, historical earthquake activity, groundwater pumping and buried ancient river channel. These factors contribute differently to the formation of earth fissures.
4. According to the lengths of earth fissures, the authors refer to a 'length-grade conversion equation' and divide earth fissures by length into 10 grades. Since earth fissures are linearly shaped, to better distinguish them on planar expressions, we designed a set of legend symbols based on the length-based fissure classification and recommend to use them in relevant researches.

Disclosure statement

No potential conflict of interest was reported by the authors.

Funding

This research was supported by the Fundamental Research Funds for the Central Universities [Grant No. 2017XKQY99] and the Project Funded by the Priority Academic Program Development of Jiangsu Higher Education Institutions (PAPD).

References

Auvinet G, Mendez E, Lermo J. 2010. *Advances in geotechnical characterization of soil fracturing in Mexico city basin*. In: CarreonFreyre, D, Cerca M, Galloway DL, SilvaCorona JJ, editors. Land Subsidence, Associated Hazards and the Role of Natural Resources Development. Wallingford, United States: *Int Assoc Hydrological Sciences*. 339:33–38.

Ayalew L, Yamagishi H, Reik G. 2004. Ground cracks in Ethiopian Rift Valley: facts and uncertainties. *Eng Geol*. 75(3):309–324.

Bankher KA, Al-Harthi AA. 1999. Earth Fissuring and LandSubsidence in Western Saudi Arabia. *Natural Hazards*. 20(1):21–42. doi: 10.1023/A:1008167913575

Brunori CA, Bignami C, Albano M, Zucca F, Samsonov S, Groppelli G, Norini G, Saroli M, Stramondo S. 2015. Land subsidence, earth fissures and buried faults: InSAR monitoring of Ciudad Guzman (Jalisco, Mexico). *Remote Sens*. 7(7):8610–8630.

Carpenter MC. 1993. Earth-fissure movements associated with fluctuations in ground-water levels near the Picacho Mountains, south-central Arizona, 1980–84. In: Dallas L Peck, editor. Washington, United States: United States Government Printing Office. US *Geol Surv Prof Paper* 497-H.

Chen XX, Luo ZJ, Zhou SL. 2014. Influences of soil hydraulic and mechanical parameters on land subsidence and earth fissures caused by groundwater exploitation. *J Hydrodyn*. 26(1):155–164.

Deng Q, Yu G, Ye W. 1987. *Study on relationship between seismic surface rupture parameters and magnitude*. Beijing, China: Earthq Press.

Deng Y, Mu H, Peng J, Leng Y, Sun Z, Xue J. 2013. Experiment research on dynamic characteristics of earth fissure belt loess in Xi'an area. In: Zhang H, Jin D, Zhao XJ, editors. *Applied Mechanics, Materials and Mechanical Engineering. Applied Mechanics and Materials*. Zürich, Switzerland: Trans Tech Publications: 138–146.

Dou AX, Wang XQ, Ding X, Wang DL. 2005. Extraction of earth fissures caused by earthquake Ms 6.8 in Bachu-jiashi area. Proceedings of IGARSS 2005, Seoul, Korea: IEEE International Geoscience and Remote Sensing Symposium, Vol.1–8; p. 5053–5055.

Fan W, Yu MH, Oda Y, Lin Y, Chen LW, Iwatate T. 2004. Fracture mechanics analysis of earth fissure. In: Kishimoto K, Kikuchi M, Shoji T, Saka M, editors. *Advances in Fracture and Failure Prevention, Parts 1 and 2*. Key Engineering Materials. Zurich-Uetikon: Trans Tech Publ Ltd.; p. 87–91.

Guo A. 2000. Statistical research on relation between surface fault width of strong earthquake and magnitude. *NW Seismol J*. 22(3):301–305.

Gutenberg B, Richter CF. 1936. Magnitude and energy of earthquakes. *Science (New York)*. 83(2147):183–185.

Haimson BC, Rummel F. 1982. Hydrofractring stress measurements in the IRDP drill hole at Reydarfjordur, Iceland. *J Geophys Res*. 87:6631–6649.

Heindl LA, Feth JH, Fletcher JE, Karl H, Peterson HB, Chler VN. 1955. Discussion of symposium on land erosion "piping". Eos *Trans Am Geophys Union*. 36(2):342.

Jachens RC, Holzer TL. 1982. Differential compaction mechanism for earth fissures near Casa Grande, Arizona. *Geol Soc Am Bull*. 93(10):998–1012.

Jingming W. 2000. *Theory of earth fissures hazard and its application*. Xi'an, China: Shaanxi Sci Tech Press.

Jishan X, Lingchao M, Haibo A, Liyang W. 2015. The bending mechanism of anping earth fissure in the Hebei plain, North China. *Environ Earth Sci*. 74(9):6859–6870.

Leonard RJ. 1929. An earth fissure in southern Arizona. *J Geol*. 37(8):765–774.

Li YL, Yang JC, Hu XM. 2000. Origin of earth fissures in the Shanxi Graben system, Northern China. *Eng Geol*. 55(4):267–275.

Nutalaya P, Yong RN, Chumnankit T, Buapeng S. 1996. *Land subsidence in Bangkok during 1978–1988*. The Netherlands: Springer; p. 105–130.

Pashley EFJ. 1961. Subsidence cracks in alluvium near Casa Grande, Arizona. *Ariz Geol Soc Dig*. 4:95–101.

Peng JB. 2014. *The disaster of earth fissures in Xi'an*. Beijing, China: Science Press.

Peng JB, Chen LW, Huang QB, Men YM, Fan W, Yan JK. 2013. Physical simulation of earth fissures triggered by underground fault activity. *Eng Geol*. 155:19–30.

Peng JB, Qiao JW, Leng YQ, Wang FY, Xue SZ. 2016. Distribution and mechanism of the earth fissures in Wei River Basin, the origin of the Silk Road. *Environ Earth Sci*. 75(8):12.

Phienwej N, Giao PH, Nutalaya P. 2006. Land subsidence in Bangkok, Thailand. *Eng Geol*. 82(4):187–201.

Qu FF, Zhang Q, Lu Z, Zhao CY, Yang CS, Zhang J. 2014. Land subsidence and earth fissures in Xi'an, China 2005-2012 revealed by multi-band InSAR time-series analysis. *Remote Sens Environ*. 155:366–376.

Rodríguez R, Armienta A, Morales P, Silva T, Hernández H. 2006. Evaluación de Vulnerabilidad Acuífera del valle de Irapuato Gto. Japami, Concyteg, IGF UNAM. Reporte Técnico il.

Wang F. 2016. *The study on the syngenetic mechanism of earth fissures – case of Weihe Basin earth fissures [Eng Master Thesis]*. Xi'an, China: Chang'an University.

Wang GY, You G, Shi B, Yu J, Li HY, Zong KH. 2009. Earth fissures triggered by groundwater withdrawal and coupled by geological structures in Jiangsu Province, China. *Environ Geol*. 57(5):1047–1054.

Wu C. 2008. *Lanform environment and its formation in North China*. Beijing, China: Science Press.

Xu H. 2008. *A study on the characteristics of Meso-Cenozoic tectonics and present seismogenic structure of the southern North China Craton*. Beijing, China: Institute of Geology, China Earthq Admin.

Xu J, Fu H, Ma X, Tang D. 2012. Mechanism analysis of tectonic-type earth fissures in Shanxi down-faulted basin. In: Chu MJ, Li XG, Lu JZ, Hou XM, Wang X, editors. CEABM 2012,

Yantai, China: *Progress in Civil Engineering, Parts 1–4. Applied Mechanics and Materials*. p. 1111–1115.

Xu L, Li S, Cao X, Somerville ID, Suo Y, Liu X, Dai L, Zhao S, Guo L, Wang P, et al. 2016. Holocene intracontinental deformation of the northern North China Plain: evidence of tectonic earth fissures. *J Asian Earth Sci*. 119:49–64.

Zhang Q, Qu W, Peng JB, Wang QL, Li ZH. 2012. Research on tectonic causes of numerous earth fissures development mechanism and its unbalance distribution between eastern and western of Weihe basin. *Chin J Geophys (Chinese Edition)*. 55(8):2589–2597.

Zhang Y, Xue YQ, Wu JC, Yu J, Wei ZX, Li QF. 2008. Land subsidence and earth fissures due to groundwater withdrawal in the Southern Yangtse Delta, China. *Environ Geol*. 55(4):751–762.

Zhang YH, Wu HA, Kang YH, Zhu CG. 2016. Ground subsidence in the Beijing-Tianjin-Hebei region from 1992 to 2014 revealed by multiple SAR stacks. *Remote Sens*. 8(8):17.